Hearing Research 342 (2016) 23–38

Contents lists available at ScienceDirect

Hearing Research

journal homepage: www.elsevier.com/locate/heares

Research paper

Impulse noise injury prediction based on the cochlear energy

Brissi Zagadou*, Philemon Chan, Kevin Ho, David Shelley

L-3 Applied Technologies, Inc., 10180 Barnes Canyon Rd., San Diego, CA 92121-5701, USA

ARTICLE INFO

Article history:
Received 13 August 2015
Received in revised form
22 December 2015
Accepted 23 February 2016
Available online 9 March 2016

Keywords:
Impulse noise standard
Acoustic test fixture
AHAAH
Basilar membrane
Parametric optimization
Logistic regression

ABSTRACT

The current impulse noise criteria for the protection against impulse noise injury do not incorporate an objective measure of hearing protection. A new biomechanically-based model has been developed based on improvement of the Auditory Hazard Assessment Algorithm for the Human (AHAAH) using the integrated cochlear energy (ICE) as the damage risk correlate (DRC). The model parameters have been corrected using the latest literature data. The anomalous dose–response inversion behavior of the AHAAH model was eliminated. The modeling results show that the annular ligament (AL) parameters are the dominant cause of the non-monotonic dose–response behavior of AHAAH. Based on parametric optimization analysis, a 40% reduction of the AL compliance from the AHAAH default value removed the dose–response inversion problem, and this value was found to be within the physiological range when compared with experimental data. The transfer functions from the new model are in good agreement with those of the human ear. A dose–response curve based on ICE was developed using the human walk-up temporary threshold shift (TTS) data. Furthermore, the ICE values calculated for the German rifle noise tests show excellent comparison with the injury outcomes, hence providing a significant independent validation of the improved model. The ICE was found to be the best DRC to both large weapons and small arms noise injury data, covering both protected and unprotected exposures, respectively. The new AHAAH model with ICE as the dose metric is adequate for use as a medical standard against impulse noise injury.

© 2016 Elsevier B.V. All rights reserved.

1. Introduction

Hearing loss from exposure to impulse noise remains one of the top medical problems for the military, resulting in huge long-term medical costs and the loss of personnel due to hearing disability. According to the U.S. Department of Veterans Affairs, 21% of nearly 7 million cases contain the pathological outcomes of auditory damage (US Department of Veterans Affairs, 2011).

A system acquisition standard (MIL-STD-1474E) was recently adopted that includes the option of using the current Auditory Hazard Assessment Algorithm for Human (AHAAH) software (Price, 2007a, 2007b; Price and Kalb, 1991), which was developed by the Army Research Laboratory (ARL), or a variant of the LAeq8 model (LIAeq100ms). Both of these models have limitations. The LIAeq100ms model has not been validated, and the AHAAH is still under a rigorous investigation for verification, validation, and improvement. However, MIL-STD-1474E is not a medical standard against impulse noise. A medical standard is needed that consistently predicts injury from both small arms and large weapon noise with accurate differentiation between HPDs to replace the historical military standard, MIL-STD-1474D (Dept. of Defense, 1979).

The American Institute of Biological Sciences (AIBS) panel (Wightman et al., 2010) recommended that a biomechanically-based model relating the noise insult to the hearing organ response be used to accurately predict auditory injury from

Abbreviations: ARU, Auditory Risk Unit; AHAAH, Auditory Hazard Assessment Algorithm for Human; AIBS, American Institute of Biological Sciences; AL, Annular Ligament; AR, Acoustic Reflex; ARL, Army Research Laboratory; ATF, Acoustical Test Fixture; BM, Basilar Membrane; BOP, Blast Overpressure Project; CI, Confidence Interval; DRC, Damage Risk Correlate; GME, Middle ear pressure gain; HPD, Hearing Protection Device; ICE, Integrated Cochlear Energy; LAeq8, Standard equivalent 8 hours equal energy model-based metric; LIAeq100ms, Equal energy model-based metric integrating the impulse over 100 ms; MIL-STD-1474D, Historical military standard; MIL-STD-1474E, System acquisition standard; OC, Organ of Corti; PPL, Peak Pressure Level; REAT, Real Ear Attenuation at Threshold; SELA, A-weighted Sound Exposure Level; SVTF, Stapes velocity transfer function; TF_{EC2ED}, Transfer function from the ear canal to the eardrum; TTS, Temporary Threshold Shift; USAMRMC, USA Military Research and Materiel Command; WKB, Wentzel-Kramers-Brillouin; Z_0, Cochlear input impedance

* Corresponding author.
E-mail addresses: Brissi.Zagadou@L-3com.com (B. Zagadou), Philemon.Chan@L-3com.com (P. Chan), Kevin.H.Ho@L-3com.com (K. Ho), David.Shelley@L-3com.com (D. Shelley).

http://dx.doi.org/10.1016/j.heares.2016.02.017
0378-5955/© 2016 Elsevier B.V. All rights reserved.

impulse noise exposures to provide a model-based standard to replace MIL-STD-1474D. The AHAAH model is an electro-acoustic model of the peripheral hearing organ simulating the traumatic response of the auditory system to impulse noise. The model includes three components: the outer ear from pinna to eardrum, the middle ear comprised of the air spaces and ossicles, and the inner ear formed by the cochlea. The three components are electro-acoustically connected to each other to allow the propagation of external noise to the cochlea (Price and Kalb, 1991).

The AIBS panel recommended continued research and development to improve the AHAAH model with rigorous validation so that it can be used as a model-based standard against impulse noise injury. While the accomplishment of the AHAAH model is recognized, controversies about some of its modeling approach and simulation results have not been resolved among impulse noise experts. For instance, the parameters of the current AHAAH model, originally developed for the cat, were assigned to the human model by assuming that cats and humans have the same ear properties, but a rigorous verification of the adequacy of these parameters was not provided. This paper presents an improved AHAAH model whose parameters have been calibrated based on human data from recent literature to correctly reproduce the human ear transfer functions. One critical aspect that is also addressed by the present study is the non-monotonic dose–response behavior of AHAAH against large weapon noise as shown in (Price, 2007b), which suggests that an exposure at higher intensity will result in lower risk of injury, although this is not supported by field data (Smoorenburg, 2001). Smoorenburg (2001) found indeed that the AHAAH model is overly compressive. Even though many biological systems are characterized by a nonlinear response, an inverted V-shaped risk curve displayed by the current AHAAH is questionable. The consistent and dramatic reduction of risk of injury as the blast intensity is increased is not substantiated by human data. On the contrary, the field data support that injury rate increases with blast intensity. Therefore, a biomechanically-based model for prediction of impulse noise injury should also be characterized by a monotonically increasing dose-response. The critical improvements to AHAAH that removes this non-monotonic dose–response behavior are presented in this paper. The modeling of the acoustic reflex (AR) is another controversial aspect of AHAAH that suggests a significant difference in auditory risk between warned and unwarned exposures but will not be addressed by this study because of the lack of available data. Instead, the unwarned exposure condition is assumed for all calculation results presented in this paper.

A method also needs to be developed to account for use of the hearing protector with the model. For unprotected exposures, AHAAH uses the free field data as model input. For protected exposures, AHAAH requires the input of ear canal data (under the HPD) as input. Although limited work has suggested the possibility of the coupling of AHAAH to a hearing protector model, the development of a generalized hearing protector model is a separate research effort that is still ongoing. The present work will show the use of an acoustical test fixture (ATF) to collect eardrum pressure as the input to AHAAH when HPDs are involved.

Two sets of historical data were used to validate the improved AHAAH model. The first set of data was collected from human volunteers exposed to simulated large weapon noise in a test series conducted by the US Army Medical Research and Material Command (USAMRMC) at the blast test site at Kirtland Air Force Base in Albuquerque, NM, commonly known as the “Walk-up” or “Albuquerque” study as part of the Blast Overpressure Project (BOP). In the Walk-up study, a range of earmuffs and earplugs were used as HPDs and injury data from over 300 volunteers were collected. The results from the AHAAH model validation against the Walk-up test data also produced the model-based dose–response curves. Historical German rifle noise data from (Brinkmann, 2000; Pfander et al., 1980) were then used to independently validate the dose–response curves.

Previous analysis of the Walk-up study data has produced an empirical model fit that confirmed that the existing impulse noise auditory criteria are overly conservative by at least 9.6 dB (Chan et al., 2001) but the extension of that to small arms conditions without HPDs has not been tested. It has long been recognized that reconciliation of empirical model fits between large weapons exposures involving HPDs and small arms exposures for unprotected ears is not easy without a validated biomechanical method to handle the HPDs. This paper demonstrates that the use of the ATF is needed to enable the model-based standard to be used for protected and unprotected noise exposures.

The objective of this paper is to present the results from a 3-year research effort to develop and validate a biomechanical model-based medical standard against impulse noise injury. The biomechanical model is based on the AHAAH model with critical improvements based on published material property data and validation against human data. This work pursues a deep and thorough research of the AHAAH model by examining every component and model parameter by going into the source code with rigorous verification against literature data. The work includes detailed evaluation of the model behavior by performing extensive parametric studies. The end goal will lead to the development of a biomechanically valid correlate for construction of a dose–response relationship using human outcome data. In addition, a test method using the ATF has been developed to collect eardrum data as model input to account for the effects of HPD attenuation and head orientation.

2. Materials and methods

2.1. The human BOP Walk-up study

The historical Walk-up study conducted by the USAMRMC produced the largest human dataset known to-date (Johnson, 1994). The data include the waveforms of simulated large weapon noise for three standoff distances (1, 3, and 5 m) from the noise source and the resulting human temporary threshold shift (TTS) data from over 300 human volunteers for five types of HPDs. The HPDs used included an intact (unmodified) earmuff, a modified earmuff with 8 tubes inserted in the cushion to reduce sound attenuation, simulating a poor fitting condition, and three earplugs (French No. 1 plug, Rucker plug, and perforated plug). The waveforms were collected in the free field using pencil gauges and also under the earmuffs with a microphone for selected subjects.

The statistical design of the Albuquerque human Walk-up study was to estimate the dose threshold for 95% protection of the subjects 95% of the time against auditory injury. Injury was defined as TTS measured 2 min after exposure exceeding 25 dB (at any frequency in the exposed ear). A typical test series consisted of exposures from one of the test distances with the test subjects fitted with one of the HPDs according to the test matrix shown in Fig. 1. For each test series, there were 7 exposure levels with the peak pressure level (PPL) increasing by about 3 dB for each higher level as shown on the left side of the walk-up matrix, and an increasing number of shots (N) were given from 6 to, 12, 25, 50, and 100 at level 6, with some groups split between levels 6 and 5 at 100 shots. The vertical and horizontal arrows indicate the progression of the Walk-up study. Beginning with 6 shots, each group of n subjects was exposed at level 1; only uninjured subjects were allowed to advance to the next level. For those subjects who passed level 7, they were exposed at level 6 with the number of shots increased from 12 to 100 following the horizontal arrow; again only

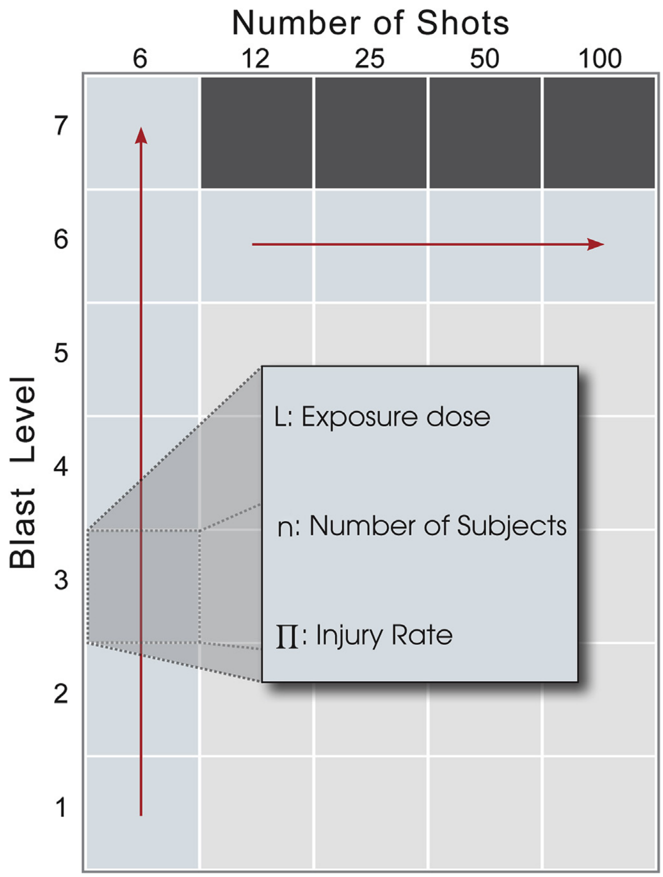

Fig. 1. Graphical illustration of the human BOP Walk-up study showing the progression through the test matrix as explained in the text.

uninjured subjects could advance to the next higher number of shots. Subjects that failed at a given level were dropped down to the next lower level and walked through the test horizontally as a side study. Each box of the matrix provides the test statistics including the number of subjects (n), the exposure dose (L), which accounts for the number of shots (N), and the injury rate (π). The Walk-up study resulted in more than 3000 outcome data points that were used in the present analysis.

2.2. *Rifle data*

The small arms data consisted of the Belgian FNC and the German G3 rifle data, for which injury data were available from (Brinkmann, 2000; Pfander et al., 1980). Table 1 summarizes the small arms data used for model validation. The injury data are given in the fourth column with the data source indicated. The German injury threshold was based on the time to recovery from TTS within 24 h rather than $TTS_2 > 25$ dB, but is generally accepted as equivalent to $TTS_2 > 25$ dB. Waveforms were obtained from input files from older versions of the AHAAH model distributed to users.

2.3. *ATF method to collect eardrum data for model input*

2.3.1. *Replication of the walk-up tests to collect ATF data*

In order to use the Walk-up data for model validation, ATF eardrum data were collected as model input by performing physical tests replicating the original conditions where the ATF devices were placed at matching locations as the volunteers in the historical tests. The commercial G.R.A.S. 45CB ANSI ATF was chosen. Matching tests for the 1 m, 3 m and 5 m conditions were conducted at the Spofford Test Site of Southwest Research Institute (SwRI) near San Antonio, TX. The test setup was replicated following the original design drawings. The charge weights for the C4 explosives used for each blast level was adjusted for the difference in altitude compared to Albuquerque, which is at 4000 ft, while Spofford is at sea level.

To quantitatively compare the original and the replicated free field waveforms, matching criteria based on the waveform characteristics were defined. When the peak level, A-duration, A-impulse defined as the integral of the positive pressure over the A-duration, and A-weighted sound exposure level (SELA) of the replicated waveform lie simultaneously within one standard deviation of the original BOP data, the two waveforms are considered matched. Thus, a series of calibration tests were performed to optimize the distance from the blast center that would satisfy the matching criteria for each test condition designated by the (nominal) distance and level. With the respective optimal distances determined, the ATF fitted with HPDs and the pencil gauges were placed at these matching distances from the blast, and the eardrum data were collected. Figs. 2 and 3 show the test setup for the 1, and 3, and 5 m tests, respectively.

The ATF eardrum data were collected in the field for all the BOP distances and levels for all HPDs with the aid of a high-end microphone (G.R.A.S. 40 BH Mic.) to collect data at the high levels. The original microphone (G.R.A.S. 40 BP Mic.) that was used to collect the data saturated at high levels.

2.3.2. *ATF data extrapolation*

Because of ATF measurement errors from microphone saturation effects at the high blast levels, the ATF data were verified for consistency before use as model input. The ATF and the human BOP undermuff pressure data trends were cross-compared based on the mean peak pressure level (PPL) versus blast level, and inconsistent data were replaced based on data extrapolation using the procedure described in Appendix A.

The criterion for data consistency was that the ATF eardrum peak pressure variation as a function of the blast level must follow the human BOP undermuff data trend. The similarity between the data trend was verified by comparing the undermuff peak pressure and the reconstructed human eardrum pressure using the transfer function from ear canal to eardrum, TF_{EC2ED}. The eardrum waveform for each exposure was reconstructed by multiplying the (protected) TF_{EC2ED} by the spectrum of the human BOP undermuff pressure data followed by applying the inverse Fourier transform to the product. The TF_{EC2ED} needed were derived from the ATF tests performed at comparable peak levels (155–160 PPL in free field) using shock tube exposures with the ATF fitted with the

Table 1
Small arms exposure data used for validation.

Rifle type	Number of waveforms	Number of shots	Injury rate (data source)
Belgian FNC (Experiment 1, 158 dB PPL)	7	6	11/51 (Brinkmann, 2000)
Belgian FNC (Experiment 2, 158 dB PPL)	7	5	9/53 (Brinkmann, 2000)
German G3 (161 dB PPL)	1	5	15% (11/78) (Pfander et al., 1980)

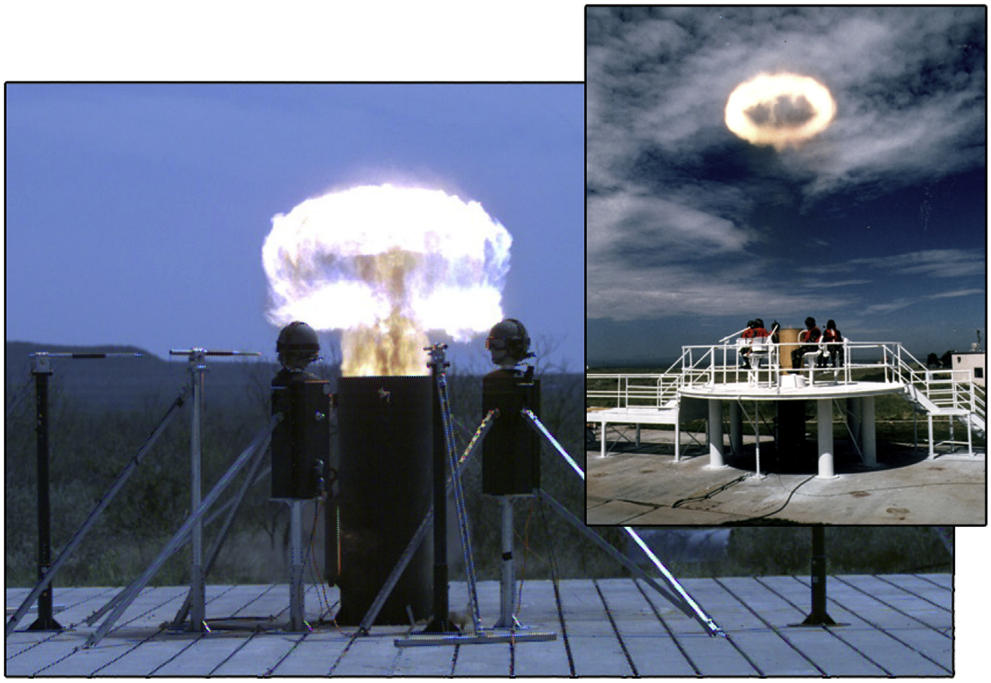

Fig. 2. 1- and 3-m test using ATF (BOP human test shown in inset). Two ATFs fitted with HPD, helmet, and goggle are shown with the right ear facing the explosion, which originates from the underground guided by a center tube. Pencil gauges shown are placed at the level of the ATFs ear at the same distance from the blast. The BOP human test shows six volunteers around the center tube with the protected right ear facing the explosion.

Fig. 3. 5-m test using ATF (BOP human test shown in inset). Two ATFs fitted with the HPD, helmet, and goggle are shown paired with pencil gauges. The explosive charge is hung above the ground between three tall cylindrical protection tubes. Similarly, the BOP human tests shows protected human volunteers with the right ear facing the explosion.

unmodified and modified earmuffs.

Hence, the ATF waveforms for the 1 m, level 7 and 5 m, level 5–7 tests were replaced with waveforms extrapolated from the lower levels following a three-step procedure. First, the lower level time domain waveforms were converted to frequency domain spectra using Fourier transform; second, the resulting frequency domain spectra were then extrapolated to the higher levels; and third, the latter were converted back to the time domain using inverse Fourier transform. The details of the waveform extrapolation procedure are described in Appendix A. The extrapolated eardrum data were verified by confirming that the peak pressure levels and waveforms were all showing increasing trends with blast level as expected similar to the undermuff pressure data.

2.4. AHAAH improvement

The AHAAH model was evaluated in depth with corrections made based on the latest literature review and model behavior analysis. The unwarned condition was adopted for model simulation for all the cases presented in this paper.

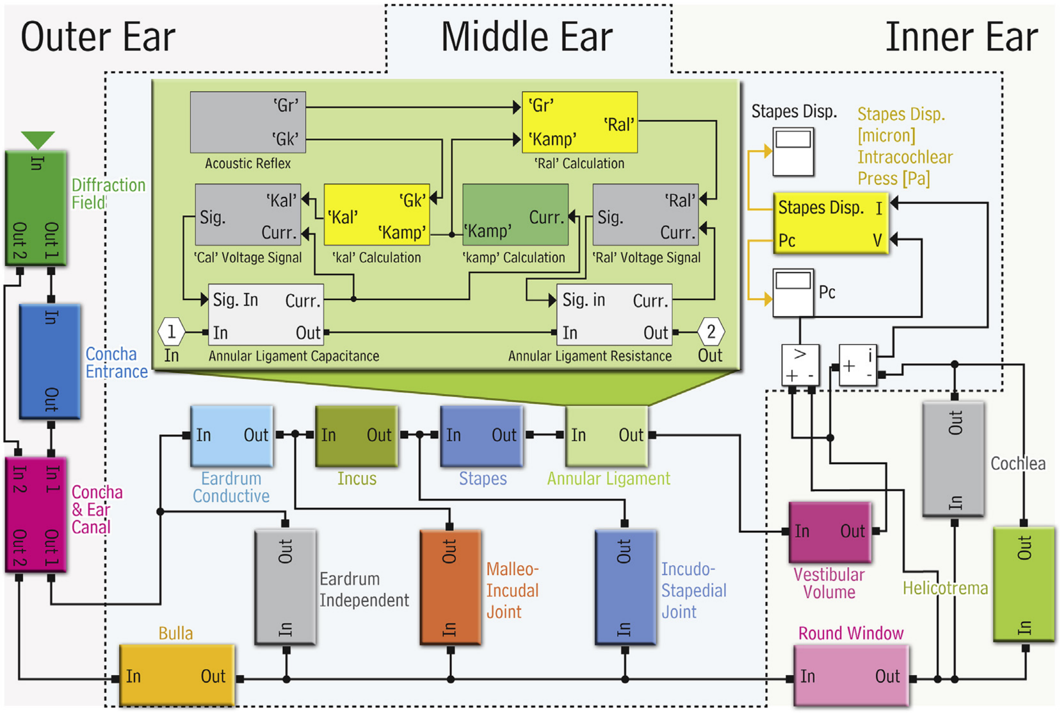

Fig. 4. Schematic of MATLAB/Simulink AHAAH model showing the hearing organ block components including the outer, middle, and inner ear. The stapes displacement (Stapes Disp.) and pressure (Pc) are collected and visualized on the scopes. The *inset* shows the details of the block for the nonlinear AL that incorporates the AR components.

2.4.1. The original AHAAH model

The MATLAB/Simulink version of the AHAAH model based on the dissertation by Song (2010) was acquired, verified and modified to produce the results presented in this paper. Fig. 4 presents a simplified block diagram of the MATLAB/Simulink version of the original AHAAH whose theoretical basis and design are briefly described here. Additional information about the original AHAAH model can be found in (Price, 2007a, 2007b; Price and Kalb, 1991). The MATLAB/Simulink version was verified by performing calculations with results matching all the published cases of AHAAH.

The AHAAH represents each part of the peripheral hearing organ from the pinna to the cochlea. Each part is represented as a set of electro-acoustic element blocks with specified parameters for the mass, compliance and resistance.

The head with the concha are modeled using a combination of two analytical approximations (Giguere and Woodland, 1994) within the network model of the analytical result for diffraction of sound by a sphere and that of the radiation impedance by a small hole in a rigid wall. The first approximation is utilized to model diffraction by a blocked piston (representing the effects of the head) using the simple network model of Bauer (1967). The second is used to model the resistance and inertance of the concha's insertion into the head. The resulting head block is characterized by the diffraction properties of the head, which are dependent on the head size.

The ear canal is modeled based on the two-tube model in (Wiener et al., 1965). The latter is based on non-dissipative plane wave propagation in ducts and gives a wavelength dependent analytical expression for the pressure at any location within the duct for a rigid eardrum boundary condition. The equivalent network model is used in AHAAH, with a straddle horn-shape added towards the concha entrance from inside the ear canal. The network model is constructed with 16 volume elements, each composed of one inductance and one compliance element.

The middle ear block starts with the eardrum, which is divided into a conductive and an independent path. The conductive path includes the portion of the eardrum attached to the malleus attachment and the handle of the malleus, while the independent eardrum is composed of the remainder of the membrane attached to the outer bony tympanic ring. Each part is characterized by their electro-acoustic elements. While all other elements of the middle ear (including the bones, joints, and the stapes) are simple and linear, the annular ligament (AL) model is nonlinear.

The AHAAH model includes two unique features of the middle ear response, the acoustic reflex (AR) and AL nonlinearities. Although complex, the protective mechanism of the middle ear AR against low frequency (<1 kHz) and high level noise is well-documented. When the timing of the noise exposure coincides with the delayed activation of the AR, it can contribute up to 20 dB decrease of the input sound level (Borg et al., 1995) in ears endowed with this special feature. Likewise, the AL nonlinearity, where the ligament displacement saturates at high PPL, has been observed in both animals and humans (Gan et al., 2011; Guinan and Peake, 1967). The incorporation of these features makes the middle ear model nonlinear and requires a time domain solution. In AHAAH, these two features are modeled together in the same simulation block as shown in the inset on Fig. 4. The AL stiffness gain 'Kamp' is nonlinearly dependent on the stapes displacement and is used to update the AL stiffness and resistance, which are modulated by the AR time dependent gain; the process is controlled through a time domain feedback loop to yield the AL impedance which determines the motion of the stapes. Based on a simplified and idealized AR gain model, AHAAH simulates the effects of warning on auditory processing. In the warned condition, when the exposed subject is aware of the incoming sound, the maximum gain of the AR is set prior to the arrival of the sound; in the unwarned condition, the maximum gain is reached with a 9 ms delay.

The cochlear model is implemented based on the Wentzel–Kramers–Brillouin (WKB) approximation that calculates the basilar membrane (BM) displacement in the frequency domain. The cochlea is connected to the middle ear through a conversion from frequency domain to time domain. The AHAAH model takes the waveform of the pressure wave in time domain as the input and allows the option for inputting the waveforms from the free field, the ear canal or the eardrum to calculate the auditory risk unit (ARU) as the damage risk correlate (DRC). ARU is calculated by summing the square of the peak upward BM displacements over the entire waveform.

2.4.2. Basis for model improvement

In the following, some of the main problems found in each module of the AHAAH model are presented as a background for the improvement effort.

In the outer ear model, it was found that given the values of the head diffraction parameters used in the AHAAH model, the human head size is underestimated by at least 35%.

The middle ear nonlinearities as implemented in AHAAH appear to be overly compressive and produce a non-monotonic dose–response behavior with blast level that is not acceptable. As reported in (Price, 2007, Fig. 2) for 1 m tests, Fig. 5 shows that as the exposure level is increased from level 1 to 7, ARU increases up to level 3 or 4 and then decreases afterward. This result suggests that exposures at high levels are safer than the lower exposure levels for the same kind of noise. Injury data show that injury rate increases with blast level (Johnson, 1994).

The physiological basis of some of the AHAAH model parameters was also questioned as a result of the verification effort. It was observed that most of the parameters were derived from chinchilla or cat data. For example, the maximum stapes displacement is set to 30 μm based on cat data (Guinan and Peake, 1967) and is equal to the AL width, which has not been adjusted for the human model. It is likely that the inaccurate model parameters contribute to the anomalous model behavior.

Major improvements to the model have been made with data comparison by (1) updating the model parameters based on the latest literature findings; (2) correcting the non-monotonic dose–response behavior with blast level; and (3) formulating a new biomechanically-based DRC.

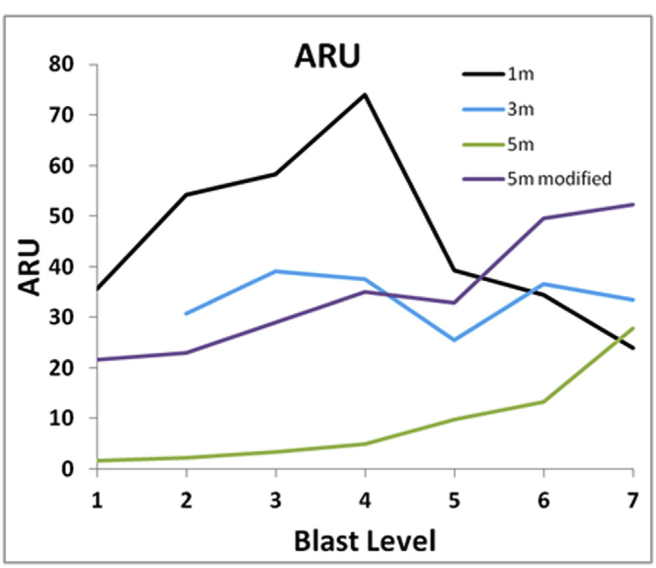

Fig. 5. AHAAH ARU versus increasing the blast level for the 1-, 3-, and 5-m tests shows that ARU produces an inverted response where higher blast levels become less damaging.

2.4.3. Model parameter update and optimization

All AHAAH model parameters were verified and updated as necessary based on latest literature findings. The model analysis showed that the dose–response behavior of the model is very sensitive to the AL parameter values, and a series of optimization calculations was carried out to determine the best value that would produce a robust dose–response behavior for the improved AHAAH model. The energy arriving at the stapes (before entering the cochlea) was used as a dose metric and the undermuff waveforms from the free field exposures from the human walk-up tests as the model input to perform the parametric optimization. The stapes energy is defined as the integral over time of the product of the pressure and volume velocity at the stapes. The ARU was also analyzed as part of the optimization effort.

Hence, the model parameters were updated in three steps. First, the parameter values as reported in the literature were used to replace those that were identified to be incorrect in the original AHAAH model. The next step consisted of optimizing the key parameters of the model to remove the dose–response inversion behavior of the model. Using Monte Carlo calculations, the AL compliance and resistance values (C_{al} and R_{al}) were optimized in an attempt to remove any dose–response inversion behavior of the model. The details of the optimization analysis can be found in Appendix B. In the final step, the converged AL compliance value was compared with the values from the literature to ensure that it is within the physiological range of the human AL values. The estimation of the AL value from the cadaver data is shown in Appendix C.

2.4.4. Verification of the improved model transfer functions

In order to verify that the final model parameters reflect the human ear transfer functions, the ear canal and middle ear transfer functions from the new AHAAH model were calculated and compared to available human data from the literature. The current AHAAH model transfer functions were also calculated for comparison. To determine the transfer functions, pure tone stimuli were successively delivered at the ear canal entrance with frequencies ranging from 0.5 to 10 kHz and peak pressure levels from 60 to 120 dB PPL, and the response at the desired point in the model was calculated.

The ear canal transfer function (TF_{EC2ED}) is defined as the ratio of the pressure at the eardrum to the pressure at the ear canal entrance. The TF_{EC2ED} from the new AHAAH model were compared to the human data from (Shaw, 1974).

The middle ear transfer functions of the new AHAAH model were compared to experimental data obtained from post-mortem human specimens (PMHS) (Aibara et al., 2001). The transfer functions are:

- Middle ear gain (GME) defined as the ratio of the intracochlear pressure (Pc) to the pressure at the eardrum (P_e)
- Stapes velocity transfer function (SVTF) defined as the ratio of the stapes linear velocity (V_s) to the pressure at the eardrum
- Cochlear input impedance (Z_0) defined as the ratio of the intracochlear pressure to the stapes volume velocity

The experiment consisted of 12 cadaver ear measurements such that the mean and standard deviations were provided. The experimental conditions were matched in the model calculations. The stimulus level and frequency were the same as for the experiment. Because cadaver data were used in the experiment, the middle ear acoustic reflex was turned off in the AHAAH model for data comparison.

2.4.5. The integrated cochlear energy

The real biomechanical meaning of ARU is unclear, and as shown later in the results ARU continues to show a dose–response inversion behavior even with the optimized AL parameters, while the stapes energy results strongly suggest that the new DRC should be energy-based. Since injury originates primarily from within the cochlea, a new DRC based on the energy deposited inside the cochlea was considered. The integrated cochlear energy (ICE) is defined as the sum of the energy accumulated over time in each of the 23 critical bands along the human cochlea, which represents the total energy deposited in the cochlea.

$$ICE = \sum_{i=1}^{23} \int_T P_i(t) V_i(t) dt \tag{1}$$

where T is the duration of the exposure, and P_i and V_i, the pressure difference across the BM and the BM volume velocity, for each location, i, respectively. The pressure difference across the BM is derived from the impedance and the volume velocity of the BM.

The BM impedance is given in terms of the BM resistance (R_{BM}), the BM compliance (C_{BM}), and the BM mass (M_{BM}), which are functions of the position (x) along the cochlea and the angular frequency (ω) of the sound pressure:

$$\begin{aligned} &Z_{BM} = R_{BM} + i\cdot\left(M_{BM}\cdot\omega - \frac{1}{C_{BM}\cdot\omega}\right) \quad \text{where,} \\ &R_{BM}(x,\omega) = R_{BM_0}\cdot\exp(-\alpha\cdot x) \\ &C_{BM}(x,\omega) = C_{BM_0}\cdot\exp(-\beta\cdot x) \\ &M_{BM}(x,\omega) = M_{BM_0}\cdot\exp(-\mu\cdot x) \end{aligned} \tag{2}$$

The BM properties assigned in the new model were identical to those in the original AHAAH model; $R_{BM0} = 912$ kg/(s m^2), $C_{BM0} = 1e\text{-}10$ m^2 s^2/kg, and $M_{BM0} = 5.8e\text{-}2$ kg/m^2 for the BM properties at the extreme base of the cochlea, and $\alpha = 1.0$; $\beta = 1.5$, and $\mu = 1.0$ for the decay constant of the BM properties.

2.5. Development of dose–response curve and threshold prediction

To develop the probabilistic dose–response curve against auditory injury and to determine the threshold of injury, calculations were performed with the improved AHAAH model using ICE as a risk factor and the ATF eardrum data from the replicated walk-up tests as the model input for all BOP free field tests. For each test group, qualified repeated eardrum waveforms were run through the new AHAAH model using the unwarned option to calculate the average ICE value. This value was assigned to each test subject within the group. To construct the binary pass/fail outcomes data table, the individual TTS data were assigned the value of 0 (no injury) for TTS < 25 dB and 1 (injured) for TTS ≥ 25 dB. A total of 3013 ICE-injury response data pairs, representing all the BOP free field data, were used in the statistical analysis. The population-average logistic regression model as implemented in (Chan et al., 2001) was used to correlate the ICE dose to the human injury outcomes to establish the dose–response curve and the L(95,95) threshold for protection of 95% of the population 95% of the time against TTS > 25 dB. Following standard logistic regression calculations, the regression coefficients were determined by fitting the ICE values with the entire human data set for all the test cases using the STATA software (StataCorp, 2009). The 95% confidence interval (CI) for the estimated probability of injury is calculated from the mean estimates and covariance matrix of the regression coefficients and by assuming a normal distribution of the error of the regression. The L(95,95) threshold is given by the upper bound of the CI with a probability of injury of 5%. A straight-forward 10-bin data grouping process was used for comparison with the dose–response curve. The binning process consists of sorting the ICE-dose in ascending order and dividing the data into 10 bins, followed by calculating an average value within each bin. The average data were compared to the mean correlation curve.

A logarithmic function of the ICE was used to express the dosage as dB. Hence, the ICE dose is expressed as:

$$Dose = 10\cdot\log_{10}\left(\frac{\langle ICE\rangle}{ICE_0}\right) + 10\log_{10}(N) \tag{3}$$

where <ICE> represents the average DRC value at each exposure level of the BOP walk-up tests. The reference value, ICE_0 represents the estimated smallest ICE value possible at 1.92e-15 μJ. For multiple shots, the dose is assumed to accumulate according to the traditional $10\log_{10}(N)$ rule, where N represents the number of shots.

2.6. Model validation

To independently test the improved model with the new DRC against different types of impulse noise, the historical small arms

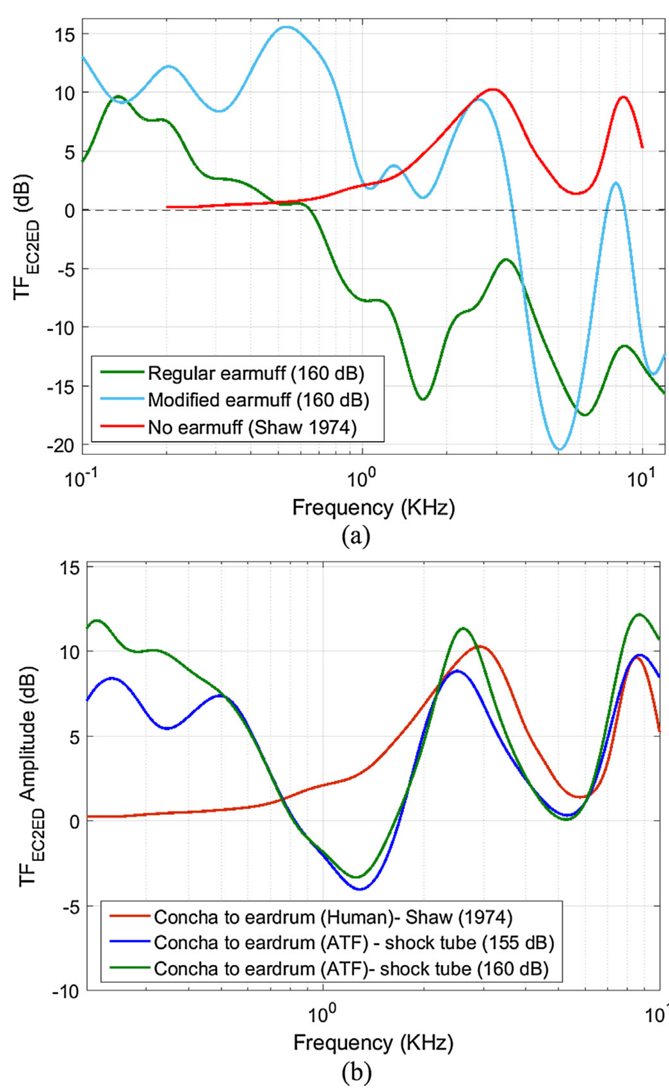

Fig. 6. TF_{EC2ED} measurement from ATF. a) with earmuff; b) without earmuff.

data were used to perform calculations for data comparison, and the results were overlaid on top of the dose–response curve obtained from the BOP large weapon data analysis.

The rifle exposures were unprotected. Therefore the waveforms were run using the free field input mode (option 1 in AHAAH). As for all of the cases presented in this paper, the unwarned condition was adopted. The available waveforms were used to calculate the average exposure dose according to Eq. (3) for data comparison.

3. Results

3.1. ATF data

This section summarizes three main results related to the ATF measurements. 1) The TF_{EC2ED} measurement results used to reconstruct the eardrum waveforms from the BOP undermuff data; 2) the trend comparison for the pressure peak and spectrum that supports data extrapolation; and 3) a sample of the complete ATF waveforms that were used as the AHAAH model input.

The TF_{EC2ED} measurement results are shown in Fig. 6. Fig. 6a shows the comparison results for TF_{EC2ED} when the ATF is fitted with unmodified and modified earmuffs. The results show that TF_{EC2ED} is not the same when the earmuffs are worn. The results also show that the TF_{EC2ED} can be very different for different earmuffs. As expected, the regular earmuff is more attenuating than the modified earmuff by up to 15 dB. For the earmuffs, there exists a crossover frequency above which there is a pressure loss as opposed to a pressure gain from the ear canal to the eardrum, and this crossover frequency is different between the modified and unmodified earmuffs. A noticeable discrepancy is observed for the low frequencies (<2 kHz), however. The TF_{EC2ED} in the presence of the earmuff do not tend to zero at very low frequencies. This seemingly unphysical characteristic was also present for the TF_{EC2ED} for the bare ATF (no earmuff) at low frequency (<2 kHz). As shown in Fig. 6b, at low frequency, the transfer function from the bare ATF deviates from that for the human, which tends to zero. A better agreement between the bare ATF and human data is found however between 2 and 10 kHz. As shown in Fig. 6b, between 2 and 10 kHz, the ATF and human measurements are in fair agreement considering the differences in noise types and intensities.

Fig. 7 shows the trend comparison between the peak pressures at the concha (undermuff) and eardrum for the 5 m tests. Fig. 7 shows that the peak pressure for the BOP undermuff and the reconstructed human eardrum pressures increased monotonically with exposure level.

Sample waveforms for the lower levels and their corresponding spectra are shown in Fig. 8 for the 1 m and 5 m tests. It can be observed that, overall, the power spectra increase with exposure level. In particular, for the 1 m tests which represent the most powerful arrival at the ear, the spectra increase up to the second highest level studied (level 6) (Fig. 8a, b). These results indicate that the eardrum waveform spectra are increasing with levels and that data extrapolation is reasonable.

Fig. 9 shows the complete ATF data used as model input for the 5 m tests with the modified earmuff. The data comprise the actual ATF data collected from level 1 to level 4 and the extrapolated data from level 5 to 7. The waveforms are all similar and become stronger as the intensity level increases. The peak of the extrapolated waveforms increased monotonically as those of the human undermuff waveforms. The same observations are made for the extrapolated waveform at level 7 for the 1 m tests.

3.2. Dose–response inversion correction

Table 2 summarizes the modification of the parameters in AHAAH based on the latest literature review findings (with citations shown in the last row). The human head size originally set to 25 cm in circumference was corrected to the average human head size of 55 cm based on anthropometric data from (USDoD, 2012). This change affects the head diffraction parameters of the model. The stapes footplate area was from 2.1e-4 m^2, a value reflecting chinchilla stapes, to 3.2e-4 cm^2 for human (Von Bekesy, 1960). The middle ear mechanical transformer ratio was adjusted from 20 to 24 based on (O'Connor and Puria, 2008). As the result of this update alone, the response inversion was removed for the 3 and 5 m tests but not for the 1 m test (Fig. 10a).

From the subsequent parameter optimization that analyzed ARU and the stapes energy in turn as the DRC, it was found that no combination of middle ear parameters could be obtained to remove the ARU dose–response inversion behavior. However, when the stapes energy was used as the DRC, the annular ligament compliance (C_{al}) was the most significant parameter, and a value of C_{al} at least 60% less than the original AHAAH value was needed to remove the inversion behavior of the stapes energy (Fig. 10b). This value was subsequently used in the improved AHAAH model as shown in Table 2.

Table 3 summarizes the results for the AL value range comparison. The results show that the AL physiological compliance value can span a wide range dependent on the experiments. The AL compliance value from (O'Connor and Puria, 2008) is large compared to (Gan et al., 2011); this value is just about outside the range predicted by the latter experiment. The AHAAH default value is close to the mean AL value found from (Gan et al., 2011) and is about one order of magnitude smaller than that from (O'Connor and Puria, 2008). The threshold of non-inverted stapes energy predicted from the sensitivity analysis corresponds to the AL compliance value of 1.96e-15 (s^2 m^4/Kg). This value is well within the experimental range of (Gan et al., 2011).

The comparison of the dose–response behavior between the ICE and ARU is shown in Fig. 11. Again, all calculations were performed for all the BOP free field series for all HPDs using the new AHAAH model with the ATF eardrum pressure data as input. Fig. 11a shows that the ICE always increases monotonically as a function of exposure level for all HPDs. As shown in Fig. 11b, ARU still inverts for both the earmuff and earplugs as the blast level is increased. The calculation results show that the ICE is the preferred DRC. Based on these results, the ICE is chosen as the DRC for validation against

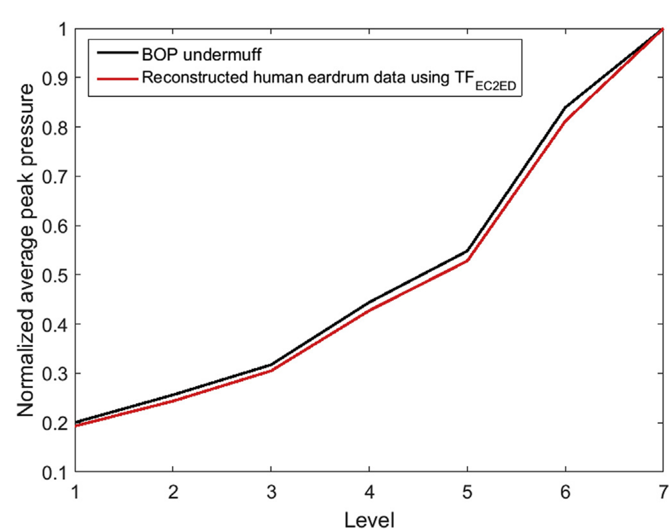

Fig. 7. Peak pressure trend comparison between BOP human undermuff and reconstructed human eardrum data (5 m tests).

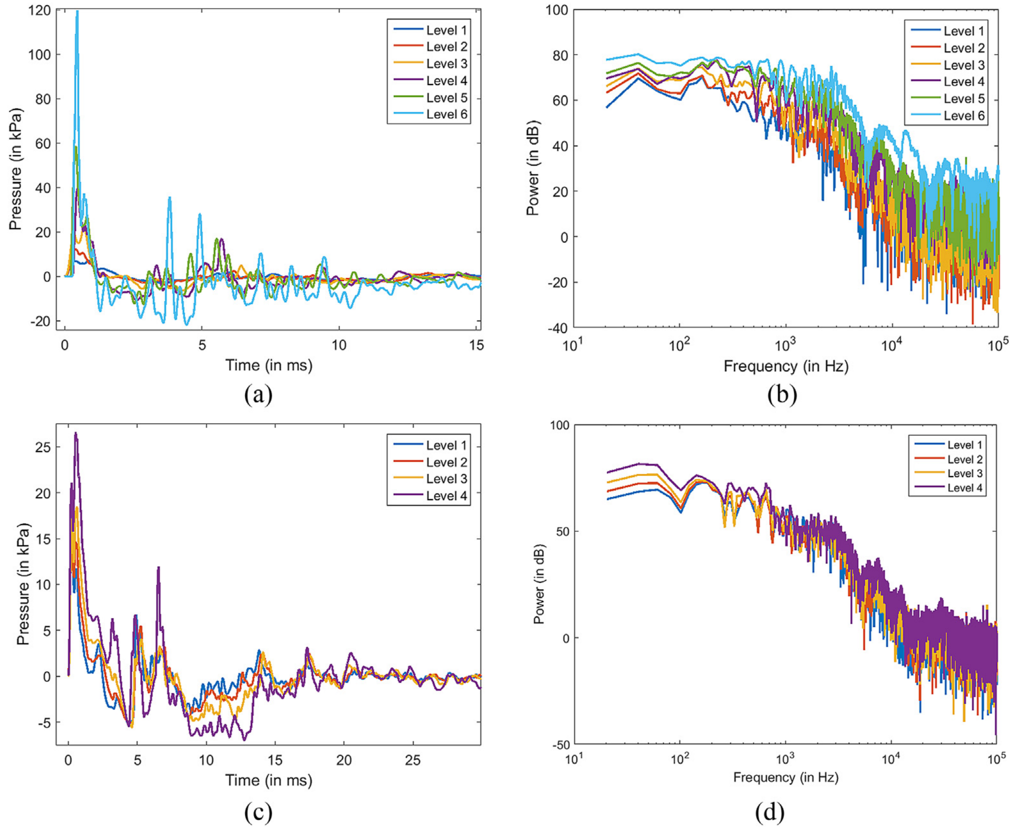

Fig. 8. ATF eardrum waveforms and spectra for low-intensity levels for 1 m and 5 m tests, modified earmuff. a) Pressure–time data, 1 m tests b) Power spectra, 1 m tests c) Pressure–time data, 5 m tests d) Power spectra, 5 m tests.

injury data to establish the dose–response curve and injury threshold.

3.3. Verification of ear transfer functions

Fig. 12 through Fig. 15 show the transfer functions comparison results. In Fig. 12, TF_{EC2ED} from the new model is compared to the human measurement by Shaw (1974). The model result is in good agreement with the human data. Also shown in Fig. 12, the transfer function obtained from the current AHAAH is similar to that from the new AHAAH model.

Fig. 13 through Fig. 15 show the middle ear transfer functions comparison results. The results presented correspond to the intensity of 60 dB across the frequency range considered since the results were practically insensitive to the intensity level.

Fig. 13 shows the middle ear gain comparison for the new AHAAH model against human data. The current AHAAH is also added for reference. Both the absolute value and the phase of GME are shown in Fig. 13. Overall, GME is within the experimental data range. In the mid-frequency range from ~1 to 5 kHz, the gain magnitude for the new model is within the human measurement error. The gain magnitude departs from the mean value for frequencies below ~1 kHz where it approaches the upper bound for the human data. Above 5 kHz, GME magnitude approaches the lower bound for the human data. It can be remarked that the current AHAAH model gain magnitude deviates significantly from the human data in the low frequency range but the new model shows better comparison. Although not closely matched across the frequency range studied, the trend for the phase of GME obtained from the new model and the human data is similar.

As shown in Fig. 14, the stapes velocity transfer function, SVTF shows an overall fair agreement with the human data. Above 7 kHz, SVTF magnitude lies within the experimental value range. Below 7 kHz, the magnitude is just outside of the measurement upper bound values. The SVTF from the new AHAAH model is in better agreement with the human data compared to the current model.

Fig. 15 shows the results for the cochlear input impedance comparison. As shown Fig. 15, the cochlear input impedance magnitude is closely matched in the new AHAAH model above 0.5 kHz. There is a slight deviation from the mean values of the measurement below 0.5 kHz, but the model results remain within the experimental value range. The phase of Z_0 is close to the upper bound of the measurement values with a phase of ~0° across the frequency range and is consistent with the fact that Z_0 is essentially resistive for high frequencies. In contrast, the current model results deviate significantly from the human measurements.

In summary, the transfer functions from the new AHAAH model show better agreements with the human data when compared to those produced by the current AHAAH model. The most noticeable differences were observed for the middle ear gain at low frequencies and the cochlear input impedance at high frequencies, and GME deviates from the mean data by as much as 10–15 dB, while the cochlear input impedance departs largely from the data above 500 Hz by more than one order of magnitude for the current AHAAH. The resistive nature of the cochlear input impedance at high frequency is not preserved in the current AHAAH model.

3.4. Dose–response curve against TTS > 25 dB from large weapon noise

The dose–response curve established against TTS > 25 dB from the large weapon noise data using the ICE as the DRC is presented in

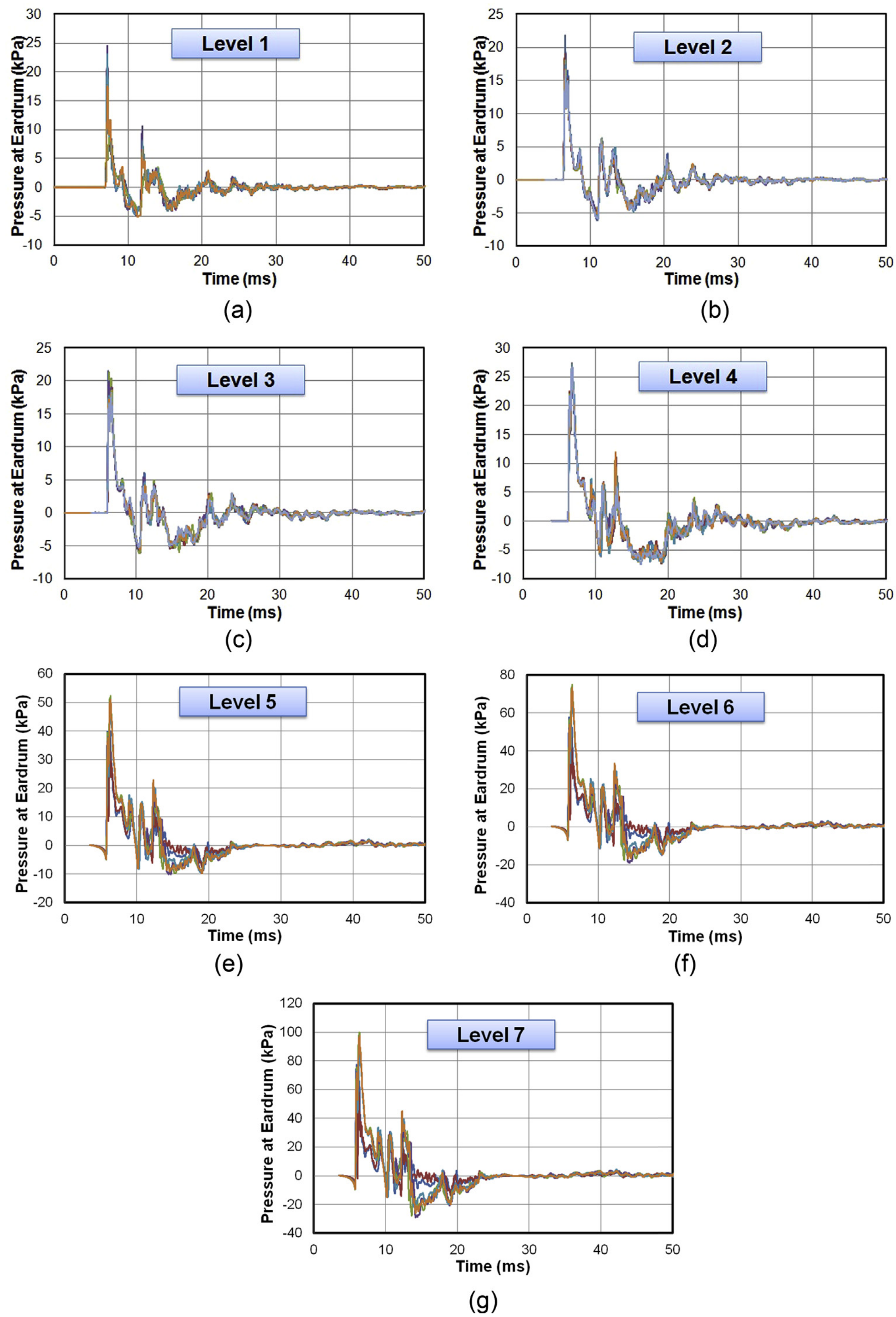

Fig. 9. ATF eardrum pressure data for the 5 m tests with the modified earmuff. (a–d) Measured waveform; (e–g) Extrapolated waveforms.

Table 2
Summary of improvement of AHAAH model parameters.

Units	Geometric parameters				Mechanical/acoustic parameters		
	Human head circumference	Stapes area	AL width, d	Mechanical transformer ratio, Nt	Cochlear input resistance	AL linear compliance	AL resistance
	m	m^2	m	unitless	kg/(s m^4)	s^2 m^4/kg	kg/(s m^4)
Current AHAAH	25e-2	2.1e-4	30e-6	20	2.64e+11	4.9e-15	2.06e+10
Improved AHAAH	55e-2	3.2e-4	70e-6	24	1.99e+10	1.96e-15	1.0e+10
Reference	USDoD (2012)	(Von Bekesy, 1960)	(Gan et al. (2011))	(O'Connor and Puria, 2008)		–	(Puria, 2003)

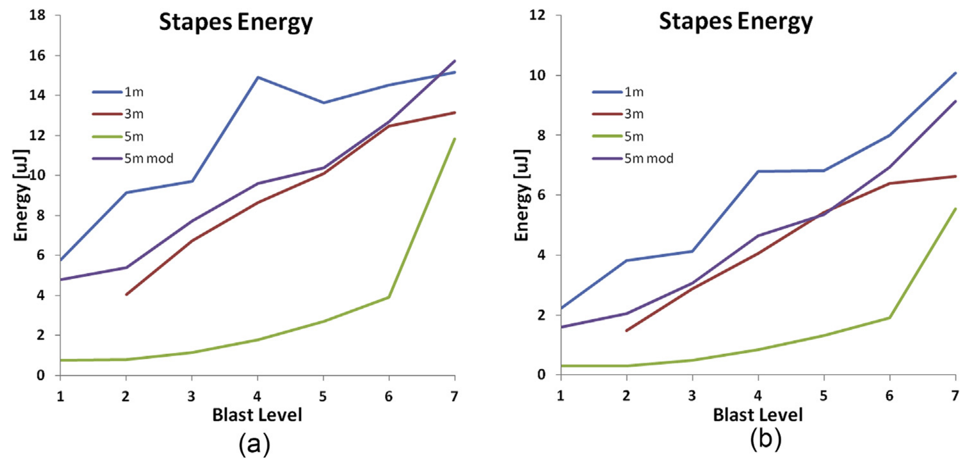

Fig. 10. Stapes energy versus the blast level to remove the dose–response behavior of AHAAH a) using the updated parameters alone b) using updated parameters with optimized AL parameters.

this section. The determination of the normalization constant for ICE is first described followed by the dose–response curve results.

The reference value, ICE_0 was estimated based on the cochlear input power threshold as follows. In humans, the power detectable at the entrance of the cochlear corresponding to the tonal threshold is 1e-12 μW (Rosowski, 1991). In the absence of energy dissipation, the power transmitted by the cochlear wave is equal to the power at the entrance of the cochlea. By definition, the power transmitted by the wave is the product of the energy per unit length of the BM and the group propagation velocity. Therefore, the energy detectable per unit length is given by the ratio of the power detectable at the entrance and the group propagation velocity, and ICE_0 can be estimated as the sum of the energy detectable per critical band of the BM. Based on the upper limit of the group velocity of 15 m/s (Lighthill, 1981) measured at low sound exposures in live squirrel monkeys, and the length of the critical band of 0.125e-2 m as assigned in AHAAH, ICE_0 was estimated to be 1.92e-15 μJ.

The dose–response curve against TTS > 25 dB established based on the large weapon noise injury data is shown in Fig. 16. The data points shown by the filled circles represent the mean failure rates based on 10-bin data grouping of all BOP data. The individual BOP injury data are shown by the cross symbols. The vertical solid line represents the dose threshold not to be exceeded for the protection against TTS > 25 dB with 5% probability of injury. The closed-black square represents the L(95,95) threshold of injury. L(95,95) is predicted at 135 dB, which corresponds to an absolute ICE threshold of N•<ICE> = 6.1e-2 μJ. There is a good fit to the binned data, and the 95% confidence interval is tight (n = 301). Therefore, the logistic regression fit and the threshold prediction are well established.

3.5. Model validation against rifle noise

Fig. 17 presents the results of the model validation against the rifle noise data with no HPD. The rifle data yield three data points that are plotted against the dose–response curve obtained from the BOP large weapon data analysis. As shown in the figure, there is

Table 3
AL compliance values comparison.

	Current AHAAH	(O'Connor and Puria, 2008)	Gan et al. (2011)	
			Min.	Max.
AL Compliance ($s^2\ m^4$/kg)	4.90e-15	12.3e-15	1.90e-15	8.88e-15

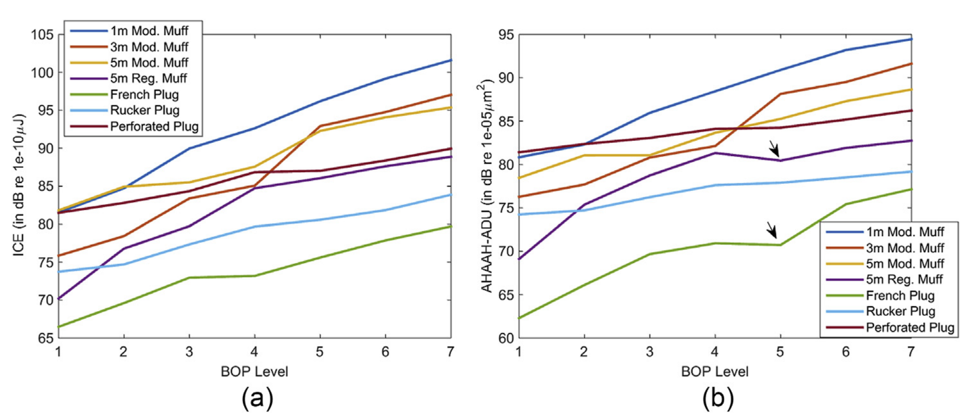

Fig. 11. DRC comparison for all BOP free field series using the ATF eardrum waveforms as model input in the new AHAAH model: a) ICE produces monotonic dose–response. b) ARU inverts as indicated by the *arrow*.

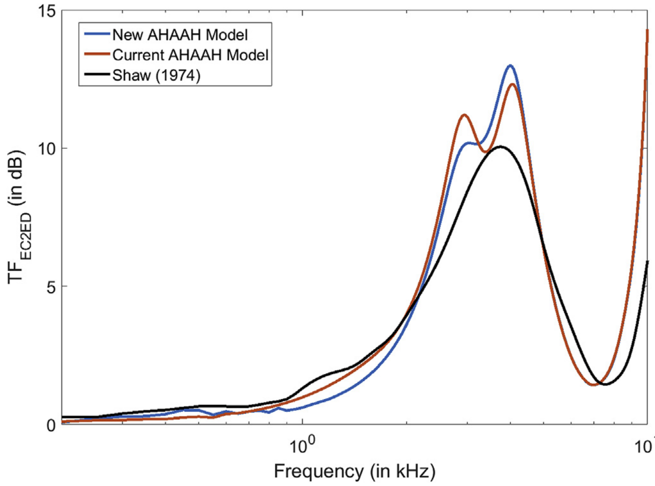

Fig. 12. Ear canal transfer function (TF_{EC2ED}) comparison. Model matches human ear canal transfer function.

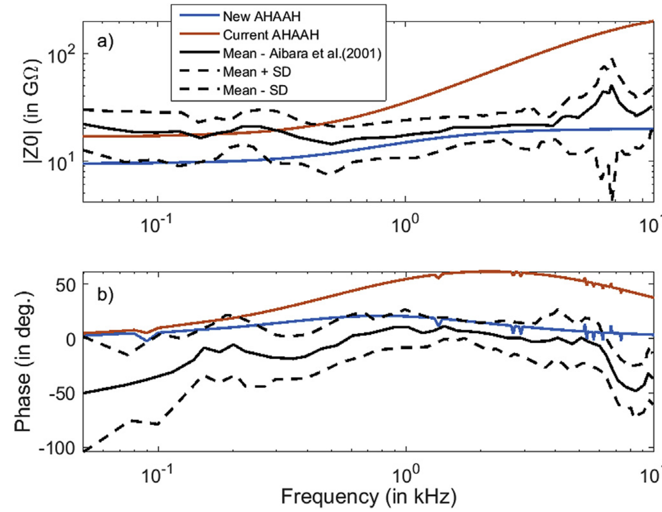

Fig. 15. Cochlear input impedance (Z_0) comparison. a) Magnitude b) Phase. New AHAAH model yields better match to human data compared to current model.

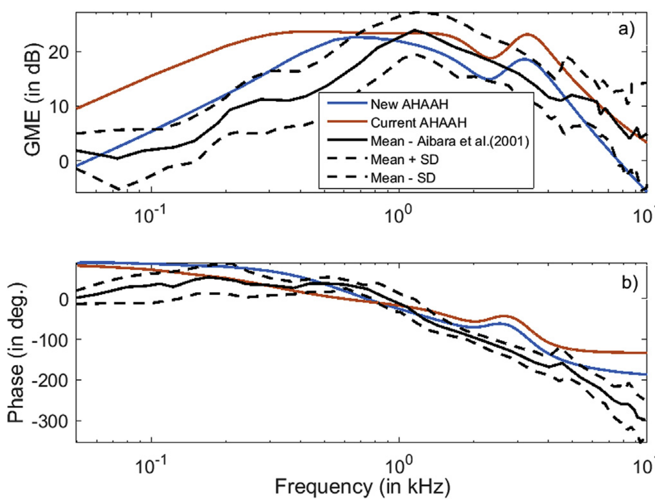

Fig. 13. Middle ear pressure gain (GME) comparison. a) Magnitude b) Phase. New AHAAH model yields better match to human data compared to current model.

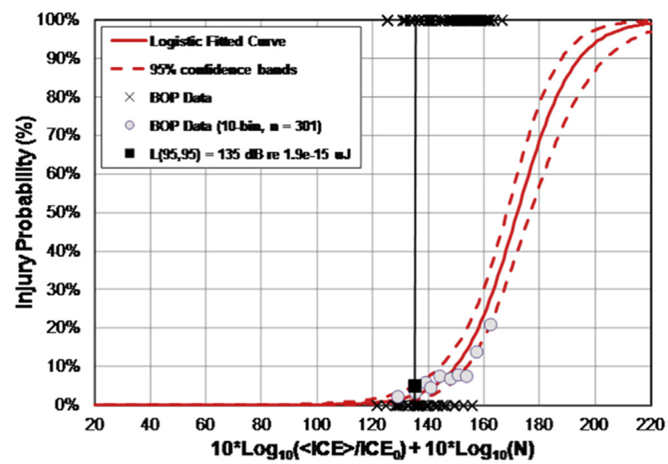

Fig. 16. Dose–response curve against $TTS_2 > 25$ dB using the large weapon noise injury data and the ICE dose as the DRC.

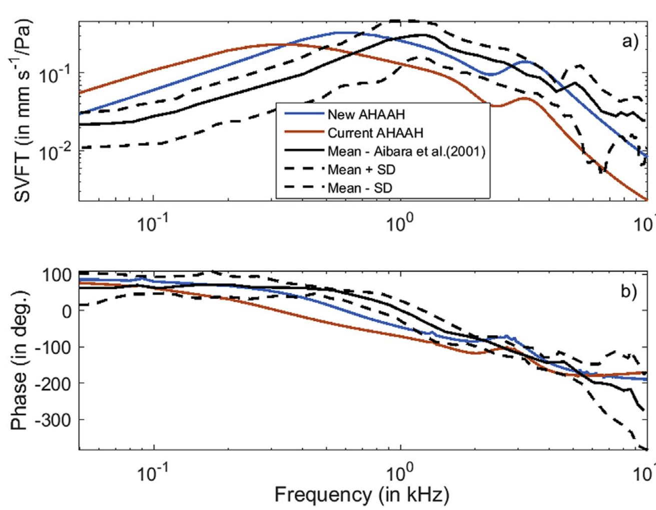

Fig. 14. Stapes velocity transfer function (SVTF) comparison. a) Magnitude b) Phase. New AHAAH model yields better match to human data compared to current model.

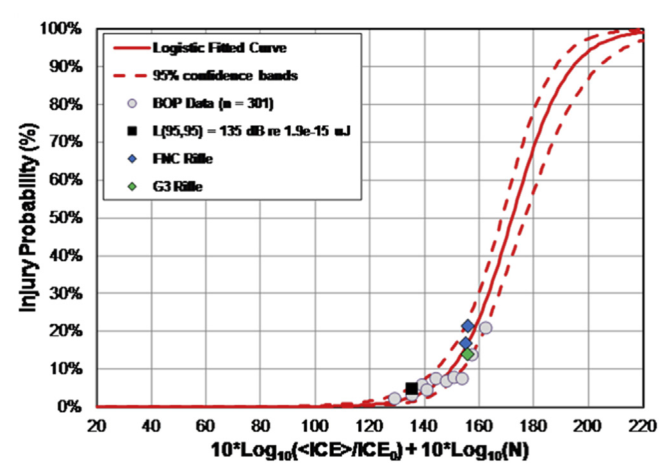

Fig. 17. Validation of the new AHAAH model against Rifle noise data.

excellent data agreement considering the diverse nature of the rifle noise injury data.

4. Discussion

This work has focused on a rigorous evaluation of the AHAAH model that resulted in a revised and improved model that can serve as a model-based auditory standard with good data comparison. The findings corroborate with the general opinions from other experts that the middle ear in the current AHAAH is overly compressive. Revisions to the model parameters including the human head size, the middle ear mechanical transformer ratio, and the AL parameters based on the latest published material data have helped correct that problem. With the development of a new DRC, the non-monotonic dose–response behavior of the current AHAAH has been corrected.

The ear transfer functions from the current AHAAH were shown to deviate noticeably from the experimental data. The consequence of such a deviation in the ear transfer functions is the introduction of errors in the model outputs. For example, for the 3 m tests with the modified earmuff, when the human BOP undermuff waveforms were run through both the new and current AHAAH, differences as high as 60 ARUs were observed between the two model outputs. These differences were on the order of the ARU values themselves, which ranged between 25 and 85 for the 3 m tests. Errors of this magnitude can lead to erroneous injury predictions. The difference between the outputs of the two models reflects the effects of the parameters change. In particular, the AL width plays an important role in controlling the amount of peak clipping in the model, and properly modeling this parameter is critical. The change from 30 μm for cats to 70 μm for humans in the new AHAAH model was significant. Also, consistent with the overly compressive behavior, the current AHAAH model always produced a lower ARU-value than the new model across all exposure levels.

It is significant to mention that this research has produced a dose–response curve that is consistent for both large weapon noise involving HPDs and small arms noise with no HPDs, which allows the setting of the correct L(95,95) threshold. The dose–response curve established using the Albuquerque large weapons noise data was independently validated by the small arms data. The apparent need for a different threshold between large weapon and small arms noise based on empirical models has been a long-time critical issue for setting impulse noise standards. This gap can only be bridged by using a model that captures the damage mechanism. This work also shows that the ICE is the correct biomechanical correlate for generating the dose–response curve.

A limitation is recognized that only two sets of human data were used for validating the model, namely the Albuquerque large weapons noise data and the German small arms data. It will be greatly beneficial to test the model with more data. Limitation of human data from well-constructed experiments has long been recognized in impulse noise research. Such efforts require the collection of pressure waveform data as well as matching auditory outcomes from test subjects under well-controlled conditions. The use of anecdotal data is not recommended for model validation.

The interpretation of the Albuquerque data has been the subject of debate within the impulse noise community. In particular, the assumption that a subject who failed at a given blast level would fail at a higher level has not been unanimously accepted. In (Price, 2007b), the injury data were altered and used to perform model validation based on a pass/fail criterion using 500 ARUs as the threshold. It is thus significant to mention that no attempt was made in the present study to alter the injury data. The injury data were used as originally reported with presumed failures in accordance to the original approved statistical protocol. A previous analysis by Chan et al. (2001) showed that predictions without presumed failures shift the threshold in the less conservative direction. It is expected that the same conclusion will be drawn from the new model without presumed failures.

A method was developed that uses an ATF to measure eardrum pressure as input to model calculations to circumvent the need for modeling the HPDs. When HPDs are worn, the interaction between the HPD and the ear in the presence of the impulse can be complex and nonlinear, thus making development of a generalized HPD model challenging. The HPD models used in the current AHAAH are based on Real-Ear-Attenuation-at-Threshold (REAT) data, which do not capture the HPD performance based on the actual exposure conditions. The insertion loss for the HPD measured using an ATF should be used instead of the REAT. During ATF evaluation, it was also found that TF_{EC2ED} is not the same when an earmuff is worn. These complexities must be reflected in HPD models. All these factors suggest that the exposure waveforms should be measured directly at the eardrum for model input to circumvent the complexity of modeling the HPDs, which in practice ultimately requires validation against ATF data. If HPDs are used, ATFs should be used to collect eardrum data as inputs to model calculations. The use of ATFs will be a necessity going forward to provide a reliable method to account for the effects of the HPDs. Because of the sophistication of new HPDs, ATF data need to be collected at the actual exposure conditions to collect eardrum data. Because of the nonlinear nature of shock waves and modern HPDs, the use of REAT to account for the insertion loss will not be recommended. The development of HPD models should be encouraged but that also requires ATF data validation at actual blast conditions.

The use of a reliable ATF microphone may strengthen the ATF testing procedure. Although collecting data at the eardrum for model input is advantageous, the ATF microphone is susceptible to saturation problems at high levels. In our analysis, data extrapolation was needed to supplement the data collected. It is possible that the extrapolated waveforms deviate from the actual waveforms at high levels. However, based on trend comparison of peak pressure level and A-weighted energy between the ATF and human undermuff (at the ear canal entrance) waveforms, the deviation in the waveforms should not affect the energy content significantly. In fact, PPL trend comparison between the ATF and human undermuff is appropriate because even though the TF_{EC2ED} amplifies the PPL to produce a higher PPL at the eardrum, the increase of the PPL with exposure intensity is preserved. In addition, the reconstructed human eardrum waveforms based on the undermuff data give peak variations that are consistent with those of the ATF eardrum waveforms. Also, the resemblance between the spectral domain extrapolated waveforms and the waveforms collected at low levels suggests that the extrapolated waveform data are representative of the high levels. It is worth noting that, unlike the earmuff data which comprise both the free field and the undermuff data, the only waveforms available for the earplugs are from the free field; and without the use of the ATF method, no eardrum data can be collected when earplugs are worn. It is expected that more advanced microphones will be available to support high-intensity blast testing.

The TF_{EC2ED} measurements using the ATF show a noticeable discrepancy for the low frequencies. As shown in Fig. 6a, the TF_{EC2ED} obtained with the ATF does not tend to zero at very low frequencies. This seemingly unphysical characteristic does not appear to come from the presence of the earmuff since it was also observed with the bare ATF measurements (Fig. 6b) and may be attributed to measurement artifacts due to microphone placements at the concha or the imperfection of the ATF. However, the similarity in TF_{EC2ED} between the ATF and humans for the meaningful frequency range as shown in Fig. 6b strengthens our confidence in using the

ATF to measure TF_{EC2ED} with HPDs, and we do not expect the discrepancy at low frequency to affect the peak pressure trend comparison results.

The biomechanical basis of the ARU as the DRC is somewhat restricted. Although cilium tip link stretching and breaking are likely during disproportionate upward BM displacements as the result of overstimulation (Price, 2007a), other structures inside the organ of Corti (OC) are also susceptible to damage. Complex vibration mode shapes have been observed within the OC where the dominant modes were not confined to the subtectorial space (Karavitaki and Mountain, 2007; Nowotny and Gummer, 2011). The hair cell is one of the softest structures found in the OC and can be strained easily. The Young's modulus is four orders of magnitude smaller than that of the cilium (Zagadou et al., 2014). As the stiff cilium deflects about the rootlet, the apical surface of the hair cell resists the motion in both directions. Hence, hair cell damage can also result under large cilium deflection. Damage to the hair cells and the cilia can reduce the efficiency of the working of the ion channels and lead to TTS (Dancer, 2004). Whether the BM moves up or down, the straining of these cells can be equally important. Thus, the use of only the upward displacements is limiting. An energy-based DRC is appropriate to capture the OC damage as a whole. Although the square of the BM displacement can be interpreted as a linear form of energy, it does not take into account the impedance of the cochlear partition.

ICE appears to be the best DRC for impulse noise injury based on the following observations. The model verification results showed that although the stapes energy did not produce a response inversion behavior, it failed to reconcile both the rifle and large weapon injury data when used as DRC. This shows that not all energy-based DRC will perform as well as ICE. The injury data used in present analysis are consistent with the ICE formulation that sums the energy over the whole cochlear spiral (Eq. (1)). In fact, the TTS data collected during the Walk-up tests were used without consideration of the cochlear frequency associated with the incurred TTS (any TTS > 25 dB was considered an injury regardless of the audiometric frequency of the TTS). After all, impulse noises are broadband noise, which excite the whole cochlear length.

Even with the revised AHAAH model, the following knowledge gaps still exist that need to be addressed by new research.

(1) There is still no model that can predict the effects of a complex mixture of noise, such as impulse noise riding on top of an intense background noise and weapon firing noise at irregular intervals with unequal intensities. How the dose accumulates for such complex mixture of noise is probably more involved than the traditional N-trading rules.
(2) The role of acoustic reflex on traumatic impulse noise effects is not well understood. Research is needed to quantify the response of acoustic reflex for the general population, and work is also needed to investigate how significant that is against impulse noise. The warned vs. unwarned predictions from the current AHAAH model has not been validated.

Other factors that must be reflected in the DRC include the interstimulus intervals and acoustic reflex dynamics. Interstimulus intervals affect the effectiveness of the acoustic reflex in multiple shots scenarios as well as the N-trading relationship. The level-dependent strength of the acoustic reflex and reflex adaptation mechanism should also be added to the model.

It is recognized that the human BOP Walk-up study data is still limited. The data simulate a limited class of blasts while the inclusion of additional weapon noise types would certainly improve the predictions. The injury data results from normally incident blast conditions only. The scarcity of human injury data thus limits the prediction capability of the model.

Although representing both earmuffs and earplugs, double protection is not simulated, and the HPDs used in the study may not represent modern HPD types. Precisely, the earmuffs used in the Walk up study which have been specifically modified to simulate poor fitting conditions do not represent modern earmuffs. While the earplugs used in the Walk-up study are similar to modern earplugs, modern earplugs appear to show different attenuation characteristics even among the same category when measured at relatively low levels. Earplugs such as the E.A.R. classic foam, E.A.Rsoft Yellow Neons foam, E.A.R. Push-Ins pod-style, and the E.A.R Ultrafit premolded earplug show differences as large as 10 dB across frequencies. This is also true for certain earmuffs such as the E.A.R Muff Model 1000, Peltor Optime 105 earmuff, and Peltor Optime 95 earmuffs. However, the response of these HPDs as measured with the same ATF but at high level impulse conditions are not known.

A few other data from the Walk-up study were not included in the present correlation study. Mainly, the reverberant exposures (Bunker data) was not included because they were not part of the tests replication efforts and thus did not have ATF eardrum data associated with them. Also not included in this study are the data outside of the paths shown by the arrows of Fig. 1 because of their very small sample size. Isolated data were deliberately excluded from this study.

More practical considerations will be needed for setting the injury threshold. It should be noted that the confidence interval shown is very tight because all data from the BOP tests were pooled together to perform the logistic regression, and the complete dataset represents a relatively large sample size of 301 ($n = 301$), coming from one single experiment. This sample size may be taken to represent the general population. However, when a training exercise is conducted, the typical sample size will be much smaller. This effect can be observed by calculating a “predicted confidence interval” using a smaller n by assuming that the variance behavior stays the same as the original correlation. One needs to keep in mind that a wider scatter of data will be expected from the outcomes of a smaller group of test subjects. A policy decision will need to be made regarding how conservative one wants to set the occupational injury threshold for practical application and system testing.

The effect of the reference for ICE, expressed in dB, is merely to shift the ICE-values by a constant $10\log_{10}(ICE_0)$. Thus, the main conclusions remain unchanged as long as the same value is used for all the waveforms. Here, ICE_0 was estimated based on the input power threshold inside the human cochlea by assuming negligible energy dissipation. When energy dissipation is not minimal, the power at the entrance of the cochlea is greater than that transmitted by the cochlear wave. In this case, the current estimate would represent the upper bound for ICE_0. Also, the upper bound for group propagation velocity was estimated from a species other than human. Therefore, the resulting ICE_0 value represents only a crude estimate that helps constrain the dB range.

5. Conclusion

The AHAAH model has been modified and improved and validated against small arms and large weapon noise injury. The model parameters, originally based on cat data were upgraded to human parameters based on recent literature data. The resulting model transfer functions show good agreement with the measured transfer functions from cadaver ears. The dose−response curve established using the ICE as the DRC and the Walk-up data shows excellent agreement with rifle noise data. The ICE was found to be the best DRC to both large weapons and small arms noise injury data, covering both protected and unprotected exposures, respectively. The new AHAAH model with ICE as the dose metric is recommended to be adopted as the biomechanically-based auditory medical standard. Use of the ATF method to collect eardrum data as model input will correctly account for the HPD and orientation effects.

Acknowledgment

This paper is based on work sponsored by the U. S. Army Medical Research and Material Command (USAMRMC) Military Operational Medicine Research Program through Defense Health Program funding, Contract No. W81XWH-12-C-0036. The opinions contained herein are those of the authors and are not to be construed as official or reflecting the views of the Department of Defense. Approved for public release on 3 August 2015 by MRMC.

Appendix A. ATF eardrum waveforms extrapolation to high levels

The extrapolation procedure to obtain the replacement waveforms for the inconsistent ATF data for the high levels as revealed by human data comparison are explained in this section.

The waveforms in time domain collected at all blast levels were organized as an L-by-K matrix, where L represents the highest blast level ($L = 7$) and K, the total number of waveforms collected for each level ($K = 6$). The rows and columns of the matrix are designated by the subscripts l and k, representing respectively the blast level numbers arranged in increasing order of blast intensity and the order of collection of the waveforms (e.g. waveform number 1 was collected first, waveform number 2, second, and so on). The extrapolation was performed with respect to the blast intensity level, i.e., along the rows for each column of the matrix to obtain the waveforms for the higher levels of interest. For a given column k of the matrix,.i.e., for the kth waveform traces collected, the time domain Fourier transform is calculated for all blast levels below the highest level (l_s) where data inconsistency was first noticed. Thus, the spectra were calculated for $l < l_s$ and extrapolated to obtain the spectra corresponding to $l > l_s$. The latter spectra were then inverse Fourier transformed to determine the extrapolated waveforms in time domain for $l > l_s$. The blast level values used for extrapolation were based on the free field data.

Matlab built-in functions were combined to perform the extrapolation in the frequency domain. The command use is summarized as $y_e = fnval(fnxtr(csaps(y,x)),x_e)$, where function *fnxtr* extrapolates the low level spectra *y* with respect to the blast levels *x* and function *fnval* retrieves the extrapolated values y_e for the desired (high) level x_e. The argument of function *fnxtr* is the cubic spline smoothing function *csaps* that performs the fit of the spectra corresponding for the lower levels. The default smoothing option was used within function *csaps*.

Appendix B. Parametric optimization of AHAAH parameters

A series of Monte Carlo optimization simulations was performed on four annular ligament parameters: Cal (annular ligament compliance), Ral (annular ligament resistance), MemMagK (acoustic reflex gain), and MemMagR (acoustic reflex gain). Eight additional parameters describing the middle ear bone properties were also examined. Parametric variability was determined using Latin Hypercube Sampling (LHS) (McKay et al., 1979; Seaholm et al., 1988). Briefly, each parameter was assigned a mean value and an uncertainty range based on literature. The parameters were each divided into *m* discrete values from the lower to upper bounds of the uncertainty range. Each parameter value was selected randomly without replacement, resulting in *m* unique sets of parameter inputs to run within the AHAAH model. The output of interest was minimum fractional change of the model response (ARU or stapes energy) with a level increase in blast exposure. A minimum fractional change less than one implies there is an inversion present in the response, while a minimum fractional change greater than one implies a monotonic dose response with no inversion. The objective is to determine if any realistic combination of parameters can correct the dose-inversion anomaly.

The dominant partial correlation coefficients of minimum fractional change obtained for ARU yielded $\rho_{Cal} = -0.2509$, $p = 0.0002$; $\rho_{Ral} = 0.1582$, $p = 0.0221$; $\rho_{MemMagR} = -0.1963$, $p = 0.0044$. The other parameters, including the middle ear bone and joints parameters were insignificant ($p > 0.1$) and hence did not correlate with inversion. For the stapes energy, AL compliance was the most significant parameter ($p < 0.0002$).

Appendix C. Derivation of AL compliance from cadaver experiment

The experiment by Gan et al. (2011) used nine PMHS to perform measurements of AL geometric and material properties. For this experiment, the AL compliance needed to be derived from data. The details of the calculation are given in the following.

The available stress–strain relationship of the AL, $\tau = \tau(\gamma)$ from (Gan et al., 2011), was used to derive the force *(F)*-displacement (u_z) relationship, from which the linear AL acoustic compliance was determined.

$$F = C \cdot h \cdot \tau(\gamma); \quad \gamma = u_z/d \tag{B.1}$$

where *d*, *h*, and *C* represent the width, height and the perimeter of the AL. The motion of the stapes within the oval window is considered the simple translational motion, u_z (Von Bekesy, 1960) during which the AL ring is then simply sheared between the stapes and the oval window wall.

The AL acoustic compliance is defined as the ratio of the volume displaced and the applied pressure. When a loading force *(F)* is applied to the stapes, the side of the AL tied to the stapes moves a distance (u_z). Since AL is also tied to the oval window, which does not move, AL undergoes a shearing motion. The volume displaced is the product of the area of the triangle with sides *d* and u_z and the AL perimeter *(C)*. Using the force-stress formula in Eq. (B.1), the acoustic compliance is obtained in terms of the mechanical compliance as in Eq. (B.2).

$$C_a = C_m \cdot C^2 \cdot d \cdot h/2; \quad C_m = u_z/F \tag{B.2}$$

The mechanical compliance, C_m is given by the slope at the origin of the force–displacement curve given obtained from Eq. (B.1).

The mean AL compliance obtained based on the mean AL dimension values is

$$\langle C_a \rangle = 5.39e - 15\left(s^2 \cdot m^4 \Big/ Kg\right).$$

Differentiation of Eq. (B.2) gives the formula for error calculation on C_a based on the standard deviation on measurements of the geometric parameters, force, and displacement of AL (Eq. (B.3)).

$$\Delta C_a = (1/2) \cdot (c_1 \cdot \Delta d + c_2 \cdot \Delta h + c_3 \cdot \Delta C + c_4 \cdot \Delta C_m), \tag{B.3}$$

where

$$c_1 = C^2 \cdot h \cdot C_m; \quad c_2 = C^2 \cdot C_m \cdot d; \quad c_3 = 2 \cdot C_m \cdot h \cdot d \cdot C; \quad c_4 = C^2 \cdot h \cdot d$$
$$\Delta C_m / C_m = \Delta F / F + \Delta u_z / u_z$$

The measured standard deviations are: $\Delta d = 1.0e\text{-}5$ m, $\Delta C = 0.73e\text{-}3$ m, $\Delta h = 4.0e\text{-}5$ m, $\Delta F = 1.0e\text{-}3$ N, $\Delta u_z = 1.0e\text{-}6$ m. The standard deviation on the AL compliance, derived by assuming 15% error on the determination of the slope near the origin, was used to estimate the range for the AL compliance values.

References

Aibara, R., Welsh, J.T., Puria, S., Goode, R.L., 2001. Human middle-ear sound transfer function and cochlear input impedance. Hear Res. 152 (1–2), 100–109 doi: S0378-5955(00)00240-9 [pii].

Bauer, B.B., 1967. On the equivalent circuit of a plane wave confronting an acoustical device. J. Acoust. Soc. Am. 42, 1095–1097.

Borg, E., Canlon, B., Engstrom, B., 1995. Noise-induced hearing loss. Literature review and experiments in rabbits. Morphological and electrophysiological features, exposure parameters and temporal factors, variability and interactions. Scand. Audiol. Suppl. 40, 1–147.

Brinkmann, H., 2000. Chapter 4. Supplementary Investigation of the German Damage Risk Criterion with the Belgian NATO Small Arms Rifle FNC Reconsideration of Effects of Impulse Noise, vol. 29. NATO Research Study Group. Panel 8, AC/243.

Chan, Philemon C., Ho, Kevin H., Kan, Kit K., Stuhmiller, James H., Mayorga, Maria A., 2001. Evaluation of impulse noise criteria using human volunteer data. J. Acoust. Soc. Am. 110 (4), 1967–1975.

Dancer, A.L., 2004. Hearing and Hearing Protection. Paper presented at the RTO-EN-HFM-111 Lecture Series on "Personal Hearing Protection including Active noise Reduction", Virginia Beach, VA, USA.

Dept. of Defense, 1979. Military Standard, Noise Limits for Army Materiel *MIL-STD-1474D*. DOD.

Gan, R.Z., Yang, F., Zhang, X., Nakmali, D., 2011. Mechanical properties of stapedial annular ligament. Med. Eng. Phys. 33 (3), 330–339. http://dx.doi.org/10.1016/j.medengphy.2010.10.022.

Giguere, C., Woodland, P.C., 1994. A computational model of the auditory periphery for speech and hearing research. I. Ascending path. J. Acoust. Soc. Am. 95 (1), 331–342.

Guinan Jr., J.J., Peake, W.T., 1967. Middle-ear characteristics of anesthetized cats. J. Acoust. Soc. Am. 41 (5).

Johnson, D.L., 1994. Blast Overpressure Studies with Animals and Man: a Walk-up Study. In: EG&G Special Projects, p. 321.

Karavitaki, K.D., Mountain, D.C., 2007. Imaging electrically evoked micromechanical motion within the organ of corti of the excised gerbil cochlea. Biophys. J. 92 (9), 3294–3316. http://dx.doi.org/10.1529/biophysj.106.083634.

Lighthill, J., 1981. Energy flow in the cochlea. J. Fluid Mech. 106, 149–213.

McKay, M.D., Beckman, R.J., Conover, W.J., 1979. A comparison of three methods for selecting values of input variables in the analysis of output from a computer code. Technometrics 21 (2), 239–245.

Nowotny, M., Gummer, A.W., 2011. Vibration responses of the organ of Corti and the tectorial membrane to electrical stimulation. J. Acoust. Soc. Am. 130 (6), 3852–3872. http://dx.doi.org/10.1121/1.3651822.

O'Connor, K.N., Puria, S., 2008. Middle-ear circuit model parameters based on a population of human ears. J. Acoust. Soc. Am. 123 (1), 197–211.

Pfander, F., Bongartz, H., Brinkmann, H., Kietz, H., 1980. Danger of auditory impairment from impulse noise: a comparative study of the CHABA damage-risk criteria and those of the Federal Republic of Germany. J. Acoust. Soc. Am. 67 (2), 628–633.

Price, G.R., 2007a. Predicting mechanical damage to the organ of Corti. Hear Res. 226 (1–2), 5–13. S0378-5955(06)00218-8 [pii]; 10.1016/j.heares.2006.08.005 [doi].

Price, G.R., 2007b. Validation of the auditory hazard assessment algorithm for the human with impulse noise data. J. Acoust. Soc. Am. 122 (5), 2786–2802. http://dx.doi.org/10.1121/1.2785810.

Price, G.R., Kalb, J.T., 1991. Insights into hazard from intense impulses from a mathematical model of the ear. J. Acoust. Soc. Am. 90 (1), 219–227.

Puria, S., 2003. Measurements of human middle ear forward and reverse acoustics: implications for otoacoustic emissions. J. Acoust. Soc. Am. 113 (5), 2773–2789.

Rosowski, J.J., 1991. The effects of external- and middle-ear filtering on auditory threshold and noise-induced hearing loss. J. Acoust. Soc. Am. 90 (1), 124–135.

Seaholm, S.K., Ackerman, E., Wu, S.C., 1988. Latin hypercube sampling and the sensitivity analysis of a Monte Carlo epidemic model. Int. J. Biomed. Comput. 23 (1–2), 97–112.

Shaw, E.A.G., 1974. Transformation of sound pressure level from the free field to the eardrum in the horizontal plane. J. Acoust. Soc. Am. 56 (6).

Smoorenburg, Guido F., 2001. Assessing Risk of Hearing Loss from Exposure to Impulse Sounds: the State-of-the-art Ultimo 2001. Soest, The Netherlands, p. 43.

Song, Won Joon, 2010. Study on Human Auditory System Models and Risk Assessment of Noise Induced Hearing Loss (Doctoral dissertation). University of Cincinnati, Cincinnati, OH.

StataCorp, 2009. Stata: Release 11. Statistical Software. StataCorp LP, College Station, TX.

US Department of Veterans Affairs, 2011. Annual Benefits Report, Fiscal Year 2010. Department of Veterans Affairs.

USDoD, 2012. MIL-STD-1472G. Department of Defence Design Criteria Standard Human Engineering.

Von Bekesy, G., 1960. Experiments in Hearing. McGraw-Hill, New York.

Wiener, F.M., Pfeiffer, R.R., Backus, A.S.N., 1965. On the sound pressure transformation by the head and auditory meatus of the cat. Acta Otolaryngol. 61, 255–269.

Wightman, F.L., Flamme, G., Campanella, A.J., Luz, G., Rosentahal, T., Gallo, S., 2010. AIBS Peer Review of Injury Prevention and Reduction Research Task Area Impulse Noise Models. American Institute of Biological Sciences.

Zagadou, B.F., Barbone, P.E., Mountain, D.C., 2014. Elastic properties of organ of Corti tissues from point-stiffness measurement and inverse analysis. J. Biomech. 47 (6), 1270–1277. http://dx.doi.org/10.1016/j.jbiomech.2014.02.025.